Journal of Atmospheric and Solar-Terrestrial Physics 71 (2009) 805–815

Contents lists available at ScienceDirect

Journal of Atmospheric and Solar-Terrestrial Physics

journal homepage: www.elsevier.com/locate/jastp

Relative importance of ozone energy transfer processes in the middle and upper atmosphere

Rafael P. Fernandez [a,*], Martin Kaufmann [b], Beatriz M. Toselli [a,*]

[a] INFIQC, Centro Láser de Ciencias Moleculares, Departamento de Físico Química, Facultad de Ciencias Químicas, Universidad Nacional de Córdoba, 5000 Córdoba, Argentina
[b] Research Center Jülich, Institute for Chemistry and Dynamics of the Geosphere, Jülich, Germany

ARTICLE INFO

Article history:
Received 20 August 2008
Received in revised form
27 February 2009
Accepted 8 March 2009
Available online 20 March 2009

Keywords:
Vibrational energy transfer
Non-LTE
Ozone vibrational temperatures
Collisional VT rate constants

ABSTRACT

The relative importance of different processes and transitions in the appearance of non-LTE populations for the fundamental levels of ozone was studied by quantifying the kinetic law of every process and transition that affect each level population. The vibrational temperatures and the relative contribution of every transition are presented as a function of altitude. The results show that the appearance of non-LTE populations for the fundamental levels is not produced by a direct imbalance between absorption and emission but as a consequence of imbalanced collisional transitions provoked by the over-population of $O_3(0\,\nu_2\,0)$ levels. This fact confirms that the relaxation cascade drives through the bending mode ν_2.

1. Introduction

Ozone plays a major role in the chemistry, composition and thermal structure of the atmosphere, particularly in the stratosphere and mesosphere constituting an essential source of heat (Brasseur and Solomon, 1984; Kaufmann et al., 2003; Gil-López et al., 2005). Its formation in the upper atmosphere is believed to proceed through a three-body recombination of atomic and molecular oxygen to produce vibrationally excited ozone $O_3(\nu_1\,\nu_2\,\nu_3)$. Its excess energy is deposited in the thermal bath only when $O_3(\nu_1\,\nu_2\,\nu_3)$ is deactivated by collisions (Rawlins and Armstrong, 1987; Rawlins et al., 1987; Mlynczak and Drayson, 1990a, b) and consequently the efficiency of heat deposition depends on the competition between collisional quenching processes and emission of radiation from $O_3(\nu_1\,\nu_2\,\nu_3)$.

At low altitudes, the high collision frequency maintains a Boltzmann vibrational energy distribution characterized by the local translational (kinetic) temperature; that is, local thermodynamic equilibrium (LTE) prevails. At high altitudes, the collision frequency is low and collisions are no longer the sole means of maintaining vibrational distributions because chemical reactions and the emission and absorption of light are also important. Thus, there is a transition from LTE at lower altitudes, where collisions are rapid, to non-LTE at higher altitudes, where radiative and chemical processes cannot be neglected (López-Puertas and Taylor, 2001). In these regions, the $O_3(\nu_1\,\nu_2\,\nu_3)$ population deviates from the Boltzmann population, and consequently it is necessary to define a vibrational temperature, which is different from the local kinetic temperature (Wintersteiner et al., 1992; Edwards et al. 1993; López-Puertas and Taylor, 2001). Consideration of non-LTE vibrational populations is of great importance in the remote sensing and satellite data validation performed by different instruments, as the Michelson interferometer for passive atmospheric sounding (MIPAS) (Fischer and Oelhaf, 1996) on board the Environmental Satellite (ENVISAT) (European Space Agency and Envisat, 2000).

The modeling of non-LTE limb spectra of ozone for the different bands has been extensively studied, for example the 9.6 μm band was modeled for the MIPAS instrument (Manuilova et al., 1998) and for the SABER instrument (Mlynczak and Zhou, 1998). The same emission band has been used to obtain ozone number density profiles using CRISTA data (Kaufmann et al., 2003). Most of the models calculate the vibrational populations by solving a statistical state equation (SSE) including chemical, collisional and radiative processes for ozone and by considering line-by-line radiative transfer at least for the fundamental bands. Even though the recombination reaction is the principal non-LTE contributor for ozone, most models suggest that the first vibrational states, $O_3(0\,1\,0)$, $O_3(0\,0\,1)$ and $O_3(1\,0\,0)$, acquire non-LTE populations controlled by radiative absorption and collisions (Manuilova and Shved, 1992; Kaufmann et al., 2003). Recently, non-LTE corrections have been also applied to the 14.6 and 4.8 μm band emissions retrieval (Gil-López et al., 2005; Kaufmann et al.,

* Corresponding authors. Tel.: +54 351 4334169/80; fax: +54 351 4334188.
E-mail addresses: rfernandez@fcq.unc.edu.ar (R.P. Fernandez), tosellib@fcq.unc.edu.ar (B.M. Toselli).

1364-6826/$ - see front matter © 2009 Elsevier Ltd. All rights reserved.
doi:10.1016/j.jastp.2009.03.004

2006; respectively). In the last case, the authors suggest decreasing the collisional rate constant k_{D2} by a factor of 3–4 to fit their simulations to the measured radiance. The strong impact that collisional rate constants have on the non-LTE ozone retrieval has already been reported (Mlynczak and Zhou, 1998; Steinfeld and Gamache, 1998). Hence, it is very important to study and to quantify the real impact that those collisional processes and other processes have on the production of non-LTE populations.

In this paper, we present a new non-LTE model for ozone in the middle atmosphere. The model determines the distribution of populations in vibrational energy states of ozone by assuming steady-state conditions and accounting for the detailed effects of chemical processes, collisions, absorption and emission of radiation on each level. In the case of ozone, this type of calculation is necessary for the prediction of mid-infrared radiation above ~60 km and therefore for the successful retrieval of ozone density from limb radiance measured by satellite instruments. Calculations of mesospheric heating rates also depend on their results. The principal purpose of the paper is to focus upon intramolecular energy transfer, e.g. to quantify the flow of energy from level to level and to determine the absolute and relative importance of each individual process and transition in the mechanism. This is important because although many rate constants describing deactivation of states by collisions are not well known, their values do affect the end results significantly. Understanding the extent to which each one does so is therefore necessary to determine the magnitude of possible errors (such as the scaling of excited states rate constant), and to point toward new laboratory measurements that would be most beneficial.

2. Non-LTE model

A new non-LTE model for ozone was developed to assess the relative importance of each transition and process in the mechanism. The SSE equation is solved by matrix inversion and includes the chemical, radiative and collisional processes (1)–(5) described in detail in Section 3.1. A total of 105 ozone vibrational energy levels up to $E \approx 6250\,\mathrm{cm}^{-1}$ is included. Only transitions that do not exchange more than one quantum per mode are considered. The structure of the model atmosphere includes 66 non-regularly spaced altitude layers between surface and 120 km constituted by N_2, O_2, O_3, O and H with pressure, volume mixing ratios and temperature profiles from a typical mid-latitudes atmosphere during daytime (ROSE model data, Marsh et al., 2001). Because most ozone bands are optically thin throughout the atmosphere, the exchange of radiation between layers can be neglected in most bands except for the fundamental ones. In this manner, the SSE equation for the excited levels can be solved without considering coupling with other altitudes (López-Puertas and Taylor, 2001). The new model was validated comparing the vibrational temperatures obtained with those calculated by the GRANADA model (Funke et al., 2002) under the same conditions.

3. Processes and transitions for ozone

The ozone molecule has three normal modes of vibration: the symmetric stretching mode ($\nu_1 = 1103.14\,\mathrm{cm}^{-1}$), the bending mode ($\nu_2 = 700.9\,\mathrm{cm}^{-1}$) and the asymmetric stretching mode ($\nu_3 = 1042.08\,\mathrm{cm}^{-1}$) (Herzberg, 1991). Each ozone vibrational level is represented by $O_3(\nu_1\,\nu_2\,\nu_3)$, where ν_i is the quantum number of vibrational excitation of mode ν_i. Throughout this paper, the $O_3(0\,0\,0)$ lowest energy level will be referred to as the ground state, while the $O_3(0\,0\,1)$, $O_3(0\,1\,0)$ and $O_3(1\,0\,0)$ lowest stretching and bending levels will be referred to as the fundamental levels. The term *process* identifies the different types of physical or chemical phenomena in which the ozone molecule is involved, while an ozone *transition* is independent of the process type and only indicates the change in vibrational state for ozone before and after the process has occurred. Because several different transitions can occur by means of only one process and because a single transition can also occur as a consequence of more than one process, it is necessary to indicate specifically the process that produces it to describe correctly each transition.

3.1. Independent processes

The following list shows all the processes considered in the model:

$$\text{Chemical production} \quad O_2 + O + M \rightarrow O_3(\nu'_1\,\nu'_2\,\nu'_3) + M \tag{1}$$

$$\text{Chemical loss} \quad O_3(\nu_1\,\nu_2\,\nu_3) + O \rightarrow 2O_2 \tag{2}$$

$$\text{Collisional deactivation} \quad O_3(\nu'_1\,\nu'_2\,\nu'_3) + M \rightarrow O_3(\nu_1\,\nu_2\,\nu_3) + M \tag{3}$$

$$\text{Light emission} \quad O_3(\nu'_1\,\nu'_2\,\nu'_3) \rightarrow O_3(\nu_1\,\nu_2\,\nu_3) + h\nu \tag{4}$$

$$\text{Light absorption} \quad O_3(\nu_1\,\nu_2\,\nu_3) + h\nu \rightarrow O_3(\nu'_1\,\nu'_2\,\nu'_3) \tag{5}$$

where M represents a third body collider, N_2 and/or O_2, $h\nu$ represents an infrared photon and the primes over the quantum numbers refer to a different vibrational state.

3.1.1. Chemical processes (1) and (2)

The temperature dependence of the global rate constant for the chemical production process (k_{CP}) has been adjusted to fit the experimental data reported by Hippler et al. (1990)

$$k_{CP} = 6.0 \times 10^{-34} \left(\frac{T}{300}\right)^{-2.3} \mathrm{cm}^6\,\mathrm{s}^{-1} \tag{6}$$

The principal uncertainty in the ozone production by three-body recombination remains in the energy distribution deposited in the excited $O_3(\nu_1\,\nu_2\,\nu_3)$ produced, which has not been experimentally determined. Different types of nascent vibrational distribution have been proposed in the literature (Rawlins and Armstrong, 1987; Rawlins et al., 1987; Mlynczak and Drayson, 1990a, b; Manuilova and Shved, 1992; Kaufmann et al., 2006) such as zero surprisal, at dissociation threshold, mode specific, etc. (see López-Puertas and Taylor, 2001 or Goussev, 2002 for a detailed discussion). However, it is likely that the vibrational energy distribution should be relatively narrowed and centered close to the dissociation limit; that is to say, the third body (M) is unlikely to carry away much energy and a broad vibrational energy distribution would require unrealistically high rotational energies in order to satisfy energy conservation (Barker, 2001). Because chemical recombination does not strongly affect the non-LTE population of fundamental levels (Manuilova and Shved, 1992; Kaufmann et al., 2003), the results presented in this work consider a narrow single level nascent distribution at $O_3(0\,0\,6)$ level, with a k_{CP} value independent of the type of collider.

The rate constant for the chemical loss process (k_{CL}) has been derived from measurements of West et al. (1976), following the model of Manuilova et al. (1998):

$$k_{CL} = \begin{cases} 8.0 \times 10^{-12}\,\mathrm{cm}^3\,\mathrm{s}^{-1}, & \text{for } O_3(0\,0\,1) \text{ and } O_3(1\,0\,0) \\ \frac{5}{7} E_{\nu 3} \frac{1.0\times10^{-14}}{1.5\times10^{-11}} 8.0 \times 10^{-12}\,\mathrm{cm}^3\,\mathrm{s}^{-1}, & \text{for } O_3(\nu_1\,\nu_2\,\nu_3),\ \nu_1+\nu_3>2 \\ & E_{\nu_3} = \nu_3 1042\,\mathrm{cm}^{-1} \end{cases} \tag{7}$$

Briefly, a fixed value is used for the fundamental stretching levels, while a simple scaling is performed for higher energy stretching levels considering only the amount of energy in mode v_3. The fundamental k_{CL} value used in the model for the stretching levels is an upper limit estimation of the maximum effect that the chemical loss reaction would have on the non-LTE populations. This reaction is at most a minor contribution (approximately 30%) to the overall O_3+O deactivation (West et al., 1978). The chemical loss for bending energy levels is not considered (see Manuilova et al., 1998; Goussev, 2002). Although there is not rationale to neglect the chemical loss for the bending mode (West et al., 1976), this pathway has not been included in our model in order to compare our results with the results from other models.

Because of the high dependence of processes (1) and (2) on the oxygen atom number density, its profile is recalculated considering the ozone photochemical equilibrium (Gil-López et al., 2005):

$$[O] = \frac{J_{O_3}[O_3] + k_H[O_3][H]}{k_{CP}[M][O_2] - k_{CL}[O_3]} \quad (8)$$

where k_H rate constant accounts for OH chemical production and the J_{O_3} photolysis rate coefficient for ozone has been calculated using a new TUV-LBL model (Fernández et al., 2007). This model was developed to calculate photodissociation constants in the upper atmosphere considering the high spectral resolution of the O_2 cross section in the Schumann–Runge bands.

3.1.2. Collisional process (3)

The collisional quenching rate constants k_{VT} (VT = vibration-to-translation) for process (3) have been extensively studied and measured for ozone at the Laboratoire de Physique Moléculaire et Atmosphérique (CNRS, France) during the late 1980s and 1990s (Ménard-Bourcin et al., 1990, 1991, 1994; Doyennette et al., 1990, 1992; Ménard et al., 1992). Even though most non-LTE models do not differentiate the temperature dependence individually for colliders N_2 and O_2, in our model individual k_{VT} temperature-dependent relations for collisions with $M = N_2$, O_2 and O_3 reported in Ménard et al. (1992) are used. The k_{VT} values for the O_3+O fundamental transitions have been taken from West et al. (1976). The collisional relaxation rate constants have been measured experimentally only for the fundamental transitions shown in Fig. 1. For transitions involving higher energy levels, the k_{VT} have to be calculated by means of some theory or scaled by a rule. In this model the k_{VT} rate constants were scaled using the Landau–Teller (LT) scaling law (Lambert, 1977), which scales the rate constant values by means of the total number of quanta in each of the stretching or bending modes (Schwartz et al., 1952; Kaufmann et al., 2006); while the k'_{VT} rate constant for the reverse transitions are calculated by detailed balance. Another way to obtain the rate constants for high-energy level transitions is by means of the Schwartz, Slawsky and Herzfeld (SSH) semi-classical theory (Schwartz et al., 1952). Even though the non-LTE model developed allows the use of both methods, the results presented in this work consider LT-scaled rate constants, so that it can be compared to the results of other models. A detailed description of the different types of collisional relaxation transitions incorporated in the model is given in Section 3.2.

3.1.3. Radiative processes (4) and (5)

The band Einstein coefficient of spontaneous emission (A) for process (4) has been calculated by means of the HITRAN 2004 molecular spectroscopic database (Rothman et al., 2005). The rotational emission coefficients for each ro-vibrational transition in HITRAN are added together by performing a weighted sum to obtain the vibrational band coefficient following López-Puertas and Taylor (2001). With the exceptions of the fundamental bands, the other ozone bands are optically thin even for paths through the whole atmosphere, thus the exchange of radiation between layers is negligible. The vibrational coefficient of stimulated absorption (B) for process (5) has been included only for the fundamental transitions because the atmosphere is optically thin for the rest of the bands (López-Puertas and Taylor, 2001). B and A values are related by the usual Einstein relations. The new non-LTE model does not include stimulated emission transitions.

3.2. Independent transitions

Fig. 1 shows the different types of fundamental transitions produced by collisional process (3). Collisional processes have been selected to describe the considered transitions because those are the ones which produce the greatest impact on the coupled

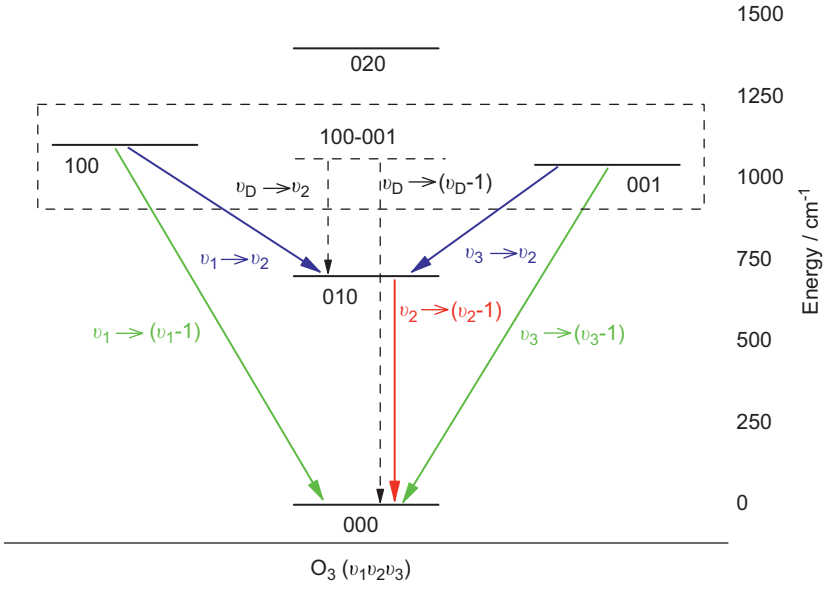

Fig. 1. Vibrational levels of ozone (horizontal lines) and their quantum numbers versus vibrational energy (in cm^{-1}). The first dyad is represented by the dashed rectangle. The arrows represent different types of collisional VT transitions: pure-stretching $v_{1,3} \rightarrow (v_{1,3}-1)$, pure-bending $v_2 \rightarrow (v_2-1)$, stretching-to-bending $v_{1,3} \rightarrow v_2$, and the experimental measured dyad transitions $v_D \rightarrow (v_D-1)$ and $v_D \rightarrow v_2$.

mechanism (SSE). Only deactivation transitions which involve a maximum change of one in the quantum number of each independent mode are presented. Even though both downward and upward transitions are produced by collisions, the description of how the energy is transferred in the atmosphere is usually explained considering only downward transitions. The transitions are classified depending on the energy variation for each vibrational mode: *pure-bending* transitions only loose one energy quantum in the v_2 mode, *pure-stretching* transitions only loose one energy quantum in the v_1 or v_3 modes and *stretching-to-bending* transitions transfer energy from modes v_1 or v_3 to mode v_2. The k_{VT} rate values for these transitions are usually referred to as k_2, k_D and k_{D2}, respectively. The strong Coriolis coupling between modes v_1 and v_3 (Doyennette et al., 1992) prevents that vibrational levels with similar excitation energy in the stretching modes could be treated independently but as members of a dyad ($v_1+v_3=v_D=1$) or a polyad ($v_D>1$). The first $O_3(1\,0\,0)$–$O_3(0\,0\,1)$ dyad is represented by the dashed rectangle in Fig. 1, and the dyad transitions measured experimentally (Ménard et al., 1992) are shown with dashed arrows. To scale higher energy transitions using the LT-scaling law, both/all independent transitions belonging to the same dyad/polyad are assumed to have the same rate constant value. For the pure-stretching transitions, it implies that the k_{VT} value for the $O_3(1\,0\,0\rightarrow 0\,0\,0)+M$ and $O_3(0\,0\,1\rightarrow 0\,0\,0)+M$ transitions is equal to the k_D fundamental rate constant measured experimentally. Although to perform the scaling of k_{VT} we have considered the dyad/polyad to which each level belongs, the SSE is set up and solved considering each mode independently. SSH theory (not considered in this paper) does not assume any dyad or polyad approximation, so k_{VT} values for v_1 and v_3 modes (for example $k_{100-000}$ and $k_{001-000}$, respectively) are calculated independently with non-equal values, being the v_3 mode values usually greater (to be submitted).

Fig. 2 shows the collisional transitions included in the model up to 4000 cm^{-1}. The main uncertainty introduced in the non-LTE model arises from the enormous amount of transitions scaled at high energies from the three fundamental levels highlighting the importance of a good scaling law. As an incorrect scaling factor will expand rapidly in the system, it is important to assess the relative importance of each transition that affects the vibrational population of each level. This is assessed by computing the kinetic law of each vibrational state in the SSE. In this way, the transitions which provoke a stronger impact on the mechanism can be identified pointing out which experimental or theoretical studies are lacking in order to improve the quality of the scaling factors included in non-LTE models. These studies will also shed light on some of the assumptions made to explain the ozone behavior at high energies.

4. Kinetics of vibrational levels

The variation in the population of each $O_3(v_1\,v_2\,v_3)$ level as a consequence of all the transitions and processes included in the model is expressed by the kinetic law defined as

$$\frac{d[O_3(v_1\,v_2\,v_3)]}{dt} = k_{CP}^{\delta i}[M][O_2][O] + \left\{\sum_j A^{ij} + \sum_j k_{VT}^{ij}[M]\right\} \times [O_3(v'_1\,v'_2\,v'_3)] - \left\{k_{CL}^{i}[O] + \sum_j A^{ji} + \sum_j k_{VT}^{ji}[M]\right\} \times [O_3(v_1\,v_2\,v_3)] \quad (9)$$

where the index i accounts for $O_3(v_1\,v_2\,v_3)$ level and the index j accounts for any other ozone vibrational level. The square brackets $[X]$ indicate the number density of the specie X. The first two terms in Eq. (9) include all the production channels, while the last term considers all the loss transitions. A^{ij} and A^{ji} are the Einstein A coefficient for spontaneous emission and are included either in the production or in the loss terms depending on whether the transition comes from a higher excited state or whether it goes to a lower energy state. In the case of fundamental transitions, A^{ij} and A^{ji} also represent the Einstein B coefficient for stimulated absorption times the mean radiance of the spectral

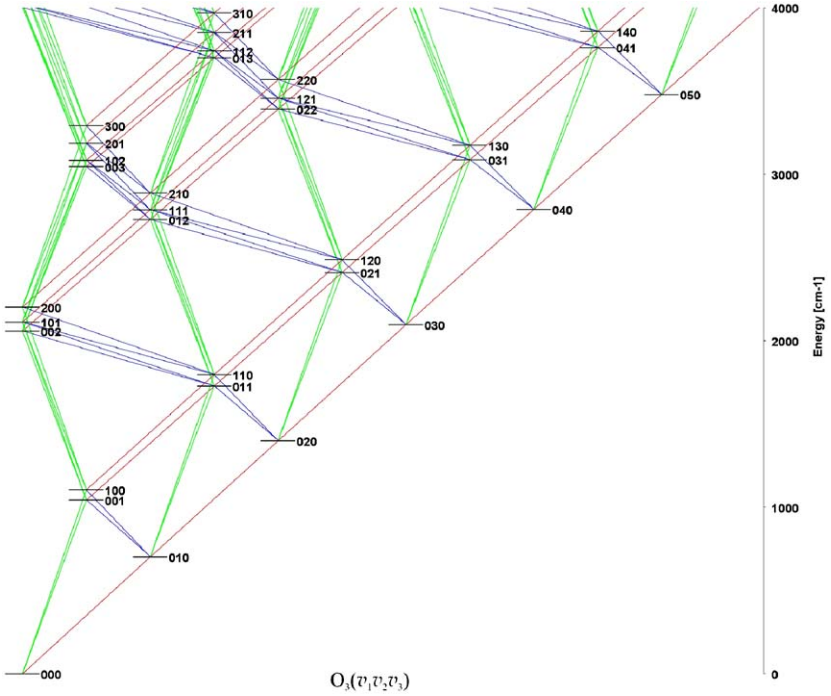

Fig. 2. Vibrational levels of ozone up to 4000 cm^{-1} (horizontal lines) and their quantum numbers versus vibrational energy (in cm^{-1}). The lines represent the different types of transitions.

band. δi considers the relative nascent distribution of vibrationally excited ozone after the three-body recombination. The reader should realize that the collisional VT summation in the loss term considers transitions that start on $O_3(v_1\,v_2\,v_3)$ level and go to any other level. Meanwhile, the equivalent summation in the production term includes transition in the opposite direction.

In order to calculate the kinetic law for every level, the SSE must be solved to obtain the non-LTE (or LTE, depending on the altitude) ozone populations for every level. After the SSE is solved, Eq. (9) is evaluated for every $O_3(v_1\,v_2\,v_3)$ level and all contributions are identified independently. Then, only the non-negligible terms are selected using a cut-off rule that can be chosen by the user depending on the type of results desired. For this work, the condition was that for every vibrational level the contribution of each transition must be at least 10^{-3} of the most important transition value affecting this level. The units of each term in Eq. (9) are molecule $cm^{-3}\,s^{-1}$.

5. Results

After the SSE is solved, the vibrational temperatures (T_{vib}) related to the vibrational populations of each level are calculated as follows:

$$T_{vib}^{O_3(v_1\,v_2\,v_3)} = \frac{E_{O_3(v_1\,v_2\,v_3)}}{k\,\ln([O_3(0\,0\,0)]/[O_3(v_1\,v_2\,v_3)])} \tag{10}$$

where the numerator is the energy of $O_3(v_1\,v_2\,v_3)$ level and the number density of all levels are referred to the $O_3(0\,0\,0)$ ground state which remains in LTE. The vibrational temperature of a certain level is the temperature that the atmosphere should have so that the population of this level equals the Boltzmann population at this altitude.

5.1. Vibrational temperatures

In Fig. 3a, the T_{vib} values obtained with the non-LTE model for the fundamental levels of ozone between 60 and 100 km are presented. Above 65 km, all fundamental levels depart from LTE presenting greater values than the local kinetic temperature (T_{kin}). The departure from LTE occurs in a three-steps sequential way as the altitude increases. First, at 65 km, the three fundamental levels depart simultaneously with the same T_{vib} value. Then, at 70 km, T_{vib} for mode v_2 deviates from T_{vib} for the stretching modes. Lastly, differences between T_{vib} values for modes v_1 and v_3 appear above 75 km. Even though between 70 and 80 km T_{vib} for mode v_2 is smaller than the ones for the stretching modes, $O_3(0\,1\,0)$ level shows a pronounced peak with greater T_{vib} values at 90 km which is discussed in the following section.

In Fig. 3b, the T_{vib} values obtained for the fundamental levels and the lowest hot levels are shown. The general profile of the hot levels is similar to those shown in Fig. 3a, but non-LTE deviations increase as the energy level increases. On the other hand, the non-LTE altitude limit decreases as the energy level increases. It is important to notice that the three-steps sequential departure explained for the fundamental levels is also observed for the hot levels differing only in the marked T_{vib} peak for $O_3(0\,2\,0)$ level which is significantly overpopulated compared to the stretching levels.

These results are usually explained considering that the collisional frequency at this altitude is low, so the importance of radiative and collisional processes is comparable in the ozone relaxation cascade after it is formed by the three-body recombination reaction (López-Puertas and Taylor, 2001). Then, every level is said to be populated or depopulated both by radiation and collision. To analyze precisely which ones are the predominant

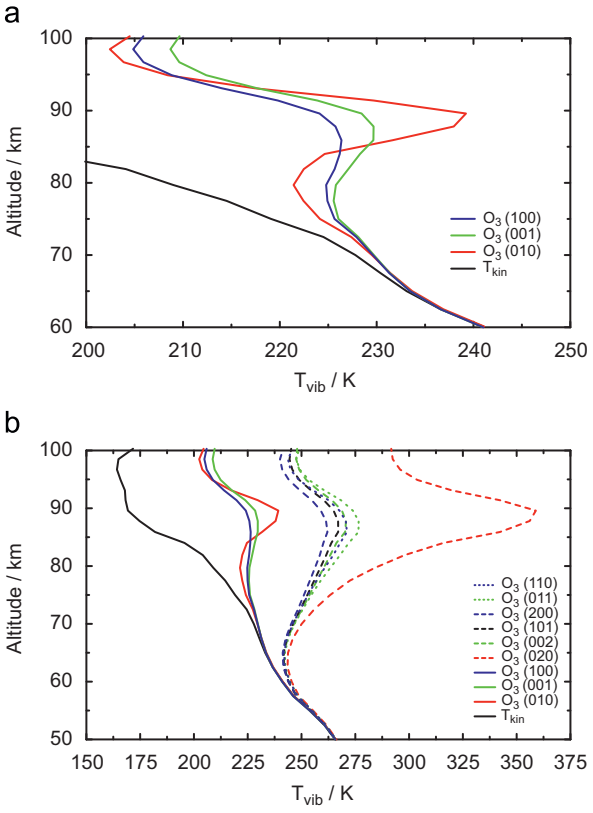

Fig. 3. Vibrational temperatures (T_{vib}) of the lower ozone energy levels as a function of altitude: (a) $O_3(0\,1\,0)$, $O_3(0\,0\,1)$ and $O_3(1\,0\,0)$ fundamental levels (solid lines); (b) $O_3(0\,2\,0)$, $O_3(0\,0\,2)$, $O_3(2\,0\,0)$ and $O_3(1\,0\,1)$ levels (dashed lines), $O_3(0\,1\,1)$ and $O_3(1\,1\,0)$ excited levels (dotted lines). T_{kin} is also shown.

terms in the kinetic law for each level, the absolute and relative importance of all non-negligible transitions have been calculated. In this manner, the impact that each transition has on the energy transfer mechanism could be quantified and analyzed as a function of altitude. This approach constitutes the distinctive characteristic of the model because it allows assessing the contribution of each transition in the relaxation cascade of ozone. Understanding the extent to which each one does so is therefore necessary to determine the magnitude of possible errors and to point toward new laboratory measurements that would be most beneficial.

5.2. Absolute and relative contribution of transitions

The absolute contribution of a given transition produced by a specific process is the correspondent right-hand side terms of Eq. (9), and is computed for all ozone levels individually once the non-LTE population for each level has been obtained. The following figures present the altitude variation of the most important transitions affecting the internal energy transfer throughout each one of the $O_3(1\,0\,0)$, $O_3(0\,1\,0)$ and $O_3(0\,0\,1)$ fundamental levels as well as the levels directly coupled to them.

5.2.1. $O_3(0\,1\,0)$ level

Figs. 4a and b show the kinetic law contribution of each transition to the population and depopulation of $O_3(0\,1\,0)$ level, respectively. In Fig. 4a, it can be seen that below 80 km, collisions with N_2 and O_2 are the most important contributors populating $O_3(0\,1\,0)$ level. The contribution of the upward transition from the ground level is significantly greater than those of the downward

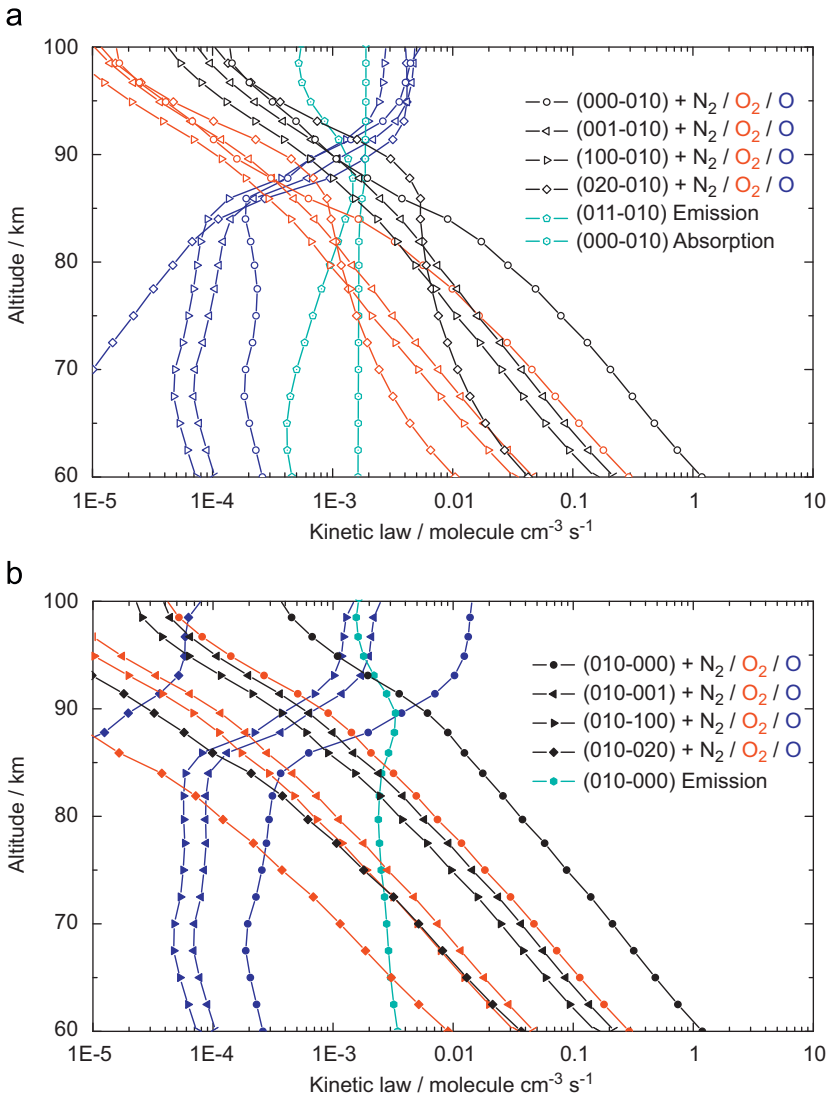

Fig. 4. Kinetic law contribution of the most important transitions affecting the population of $O_3(0\,1\,0)$ level between 60 and 100 km: (a) populating transitions (empty symbols) and (b) depopulating transitions (filled symbols). Symbols represent the different types of transitions described in the text: circle (fundamental pure-bending), triangles (fundamental stretching-to-bending) and rhombus (first excited pure-bending). Different colliders are indicated in the figure.

transitions from the higher excited states, both for N_2 and O_2. What is more, the shape of the altitude profile for the VT collisional processes for these two species is quite similar, which explains the assumption made by other models that consider both processes together (e.g., Kaufmann et al., 2003, Gil-López et al., 2005). Even though the k_{VT} rate constants for collisions when O_3 is the collider are more effective than the ones for N_2 or O_2, the contributions of these processes to the kinetic law are negligible at all altitudes because of the small ozone density. Above 85 km the oxygen atom density calculated by photochemical equilibrium increases significantly and hence collisions with atomic oxygen become more important than collisions with N_2 and O_2. Only at these altitudes, the radiative processes (4) and (5) acquire significant importance being always the absorption of radiation from the ground level more important than the emissions from the upper levels. These facts account for the marked peak in the T_{vib} value at 90 km shown in Fig. 3a. Also, it is important to note that before collisions with the O atom become the most important process, at around 90 km the downward collisional contribution from $O_3(0\,2\,0)$ level starts to dominate.

The contributions for the depopulating transitions shown in Fig. 4b are quite similar to those described in Fig. 4a, mainly for the collisions with N_2 and O_2. The major differences are: (i) that the contribution of the $O_3(0\,1\,0 \rightarrow 0\,2\,0)+M$ upward transition is always smaller than any other of the collisions shown, and (ii) that from all collisional processes with an O atom, only the $O_3(0\,1\,0 \rightarrow 0\,0\,0)+O$ downward transition shows a significant magnitude above 90 km. Once again, the radiative processes have its greater contribution at 90 km where only the fundamental emission to the ground level has a significant value.

In Fig. 5, the populating transitions presented in Fig. 4a with empty symbols and the depopulating transitions of Fig. 4b with filled symbols are shown together. Because the altitude variation of the kinetic law for O_2 collisions is similar to those with N_2, only the last ones are presented. When the contributions of the most important pairs of opposite collisional transitions are balanced, the $O_3(0\,1\,0)$ population follows a Boltzmann distribution and LTE prevails. If at least one of them is out of balance, the population of $O_3(0\,1\,0)$ level can deviate from LTE depending on the relative importance of the imbalanced transition in the whole coupled

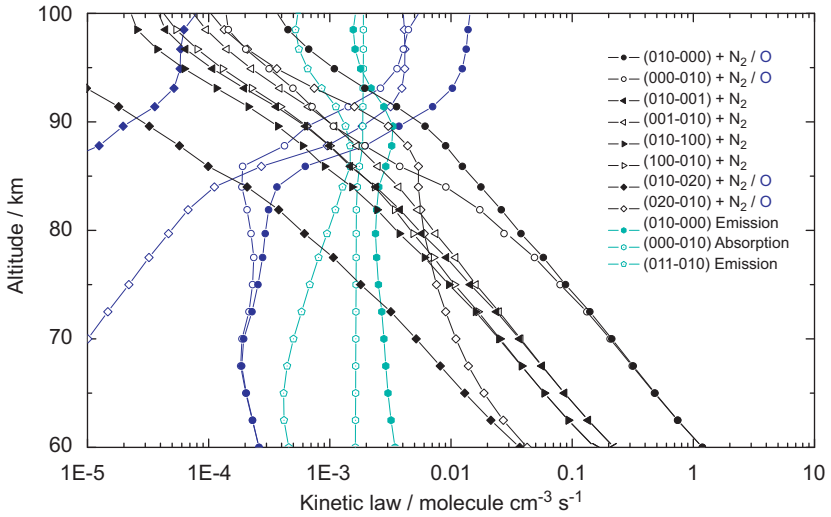

Fig. 5. Kinetic law contribution of the most important transitions populating (empty symbols) and depopulating (filled symbols) $O_3(0\,1\,0)$ level as a function of altitude. See Fig. 4 caption for reference. O_2 collisions and stretching-to-bending transitions for the oxygen atom are not included because they show a similar profile.

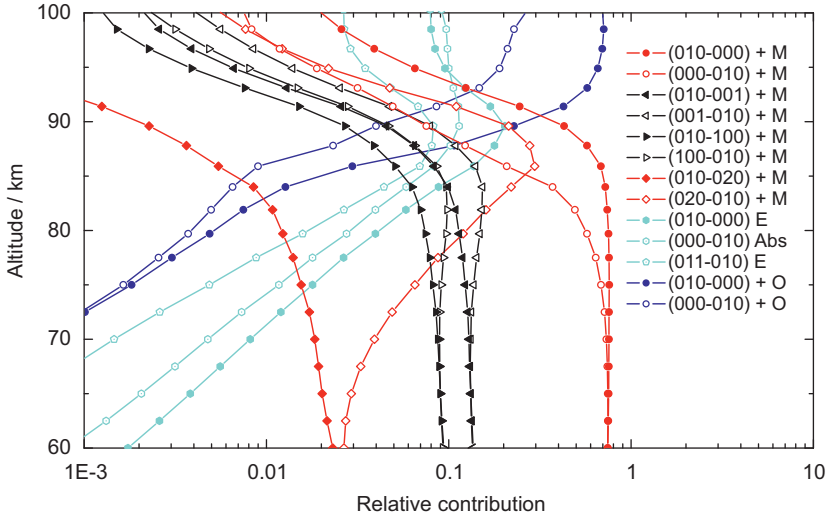

Fig. 6. Relative contribution of transitions populating (empty symbols) and depopulating (filled symbols) $O_3(0\,1\,0)$ level as a function of altitude. N_2 and O_2 collisions have been added together and are referred to as *M*. Symbols reference are as in Figs. 4 and 5. *E* stands for emission and Abs for absorption.

mechanism. In this case, below 70 km only the $O_3(0\,2\,0 \rightarrow 0\,1\,0)$+$N_2$ pure-bending collision is imbalanced and is the responsible for the initial departure of T_{vib} for all the fundamental levels.

To assess the impact of these transitions on the population of $O_3(0\,1\,0)$ level, the relative contribution of each transition calculated as the ratio between each term of Eq. (9) and the sum of all production/loss terms in the kinetic law for $O_3(0\,1\,0)$ is presented in Fig. 6. Because collisions with N_2 and O_2 have a similar effect, their contributions are added together. Here the imbalance between upward and downward transitions can be assessed clearly. At 65 km, the $O_3(0\,2\,0 \rightarrow 0\,1\,0)$+*M* downward transition is markedly imbalanced and accounts for 3% of the total energy flow of $O_3(0\,1\,0)$ level, producing its original T_{vib} departure. Because stretching-to-bending transitions are still balanced up to 70 km, there is not further non-LTE T_{vib} deviation for ν_1 and ν_3 modes, hence the stretching levels originally depart from LTE as a consequence of their collisional coupling to $O_3(0\,1\,0)$ level. There are no direct radiative processes involved at this time, so the appearance of non-LTE for all fundamental levels is only a consequence of imbalanced collisional transitions in the SSE.

The reader should notice that the imbalances shown in Fig. 6 are a consequence of the net energy transfer from the upper levels to the ground state in a deactivating downward cascade throughout $O_3(0\,\nu_2\,0)$ levels. Transitions from levels above $O_3(0\,1\,0)$, such as $O_3(0\,2\,0)$ or $O_3(0\,0\,1)$, have a greater non-LTE populating contribution (empty symbols), while the depopulating contribution is greater for the imbalanced transition to the ground state. This fact has been previously postulated by Mlynczak and Zhou (1998) and confirmed by Kaufmann et al. (2006).

5.2.2. $O_3(0\,0\,1)$ and $O_3(1\,0\,0)$ levels

In Fig. 7, the absolute contributions of the most important transitions involving $O_3(0\,0\,1)$ level are shown. The results for $O_3(1\,0\,0)$ level are very similar and are not shown. In both cases, the intermode coupling between modes ν_1 and ν_3 is at least two orders of magnitude greater than the rest of the transitions (with the exception of absorption of radiation above 90 km) and always remains completely balanced. This fact confirms the accurateness of grouping them in a dyad (e.g., Ménard-Bourcin et al., 1990,

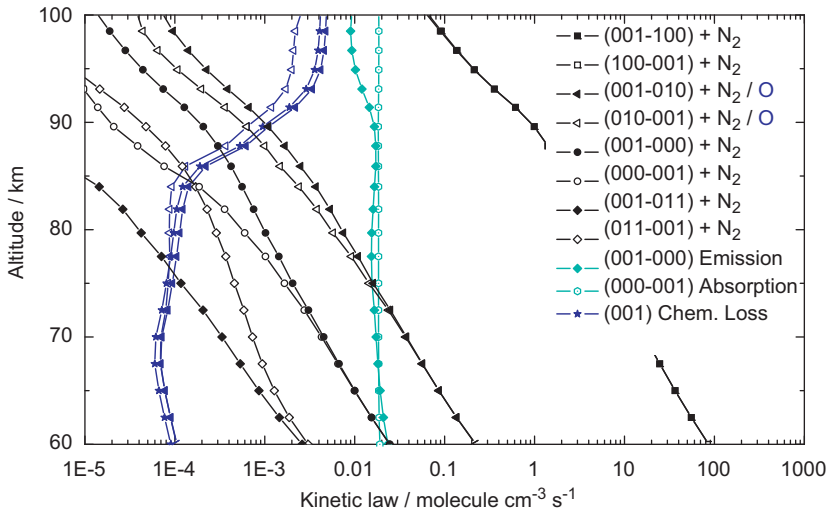

Fig. 7. Same as in Fig. 5, but for $O_3(0\,0\,1)$ level. Star symbols and square symbols represent the chemical loss process and the $v_1 \leftrightharpoons v_3$ intermode coupling, respectively.

1991; Manuilova and Shved, 1992), and explains the similarities of the T_{vib} profiles for both levels when non-LTE is appearing at 65–70 km. Also, in both cases, and differing from $O_3(0\,1\,0)$ level, the pure-stretching contributions of transitions from/to the ground state are always smaller than the stretching-to-bending from/to mode v_2 transitions. Once again, O_2 collisions are not presented because they show a similar altitude shape as the O_3–N_2 collisional contributions.

The relative contribution of the most important transitions for $O_3(0\,0\,1)$ and $O_3(1\,0\,0)$ levels are presented in Fig. 8a and b, respectively. Here, the intermode $v_1 \leftrightharpoons v_3$ coupling has not been included in the VT summation of Eq. (9) to calculate the relative values because it is by far the dominant process and always remains in LTE. The most important difference is that in Fig. 8a the radiative transitions become the most important contributor above 75 km, while in Fig. 8b their contribution increase significantly only around 85 km. When non-LTE begins for $O_3(0\,0\,1)$ and $O_3(1\,0\,0)$ levels at 65 km the stretching-to-bending transitions are balanced and are the most important contributors to the population of both levels. However, these transitions become imbalanced above 70 km which explains the second step in the T_{vib} departure sequence shown in Fig. 3a; that is, both stretching levels acquire a non-LTE population while keeping an internal LTE relationship because of the strong intermode coupling. Only above 75 km when the radiative processes for $O_3(0\,0\,1)$ become the dominant contributors, a difference in the T_{vib} value between stretching modes can be observed.

The chemical loss process for the fundamental stretching levels is as important as the VT collisions with the O atom and is for $O_3(1\,0\,0)$ level the second most important contributor above 90 km. This loss mechanism has not been considered for the bending mode and usually becomes even more important than the VT collisions with N_2 and O_2 above 85–90 km. Therefore, the marked T_{vib} peak for $O_3(0\,1\,0)$ and $O_3(0\,2\,0)$ levels might also be attributed to the absence of chemical loss process for $O_3(0\,v_2\,0)$ levels.

5.2.3. $O_3(0\,2\,0)$ level and $O_3(0\,1\,1)$–$O_3(1\,1\,0)$ dyad

Despite the fact that $O_3(0\,2\,0)$ is not a fundamental level, it plays a relevant role in the appearance of non-LTE on the fundamental levels. Also, its importance has been observed after retrieving data from MIPAS (Kaufmann et al., 2006), where the lower bending mode energy levels obtained are usually over-populated in comparison to v_1 and v_3 levels with similar energy (see Fig. 3b). The relative contributions for $O_3(0\,2\,0)$ level presented in Fig. 9 show a notable imbalance in the two most important contributors in the pure-v_2 downward cascade below 90 km: the pure-bending collisional VT energy transfer from/to $O_3(0\,3\,0)$ level and to/from $O_3(0\,1\,0)$ level. The imbalance in these transitions is the reason for the initial T_{vib} departure of the hot levels at 55 km shown in Fig. 3b. Once again, the contribution of radiative processes is not important below 75 km therefore the appearance of non-LTE for $O_3(0\,2\,0)$ level only involves collisional VT processes.

Note that the stretching-to-bending transitions to $O_3(0\,1\,1)$ and $O_3(1\,1\,0)$ levels are practically balanced up to 75 km where the upward contribution surpasses the downward one. This is an unusual case because energy is being transferred in the upward direction as a consequence of the enormous non-LTE population of $O_3(0\,2\,0)$ level that counteracts the exponential Boltzmann energy factor of the reverse k'_{VT} calculated by detailed balance. Then, the stretching-to-bending transitions that generally transfer energy to mode v_2, in this case, and as a consequence of the overpopulation, can overtake the ozone levels energy difference and transfer energy from the bending mode to the stretching modes. To the best of our knowledge, all non-LTE models described so far in the literature do not consider downward bending-to-stretching transitions in their mechanism probably because no experimental data are available. Therefore, the overpopulation of $O_3(0\,v_2\,0)$ levels is a natural consequence of the relaxation mechanism used which does not allow the energy that reaches the bending modes to return to the stretching levels.

To emphasize the impact that the mode v_2 overpopulation has on the energy flowing to the stretching modes, Fig. 10 shows the relative contributions of these transitions to $O_3(0\,1\,1)$ level (the results for $O_3(1\,1\,0)$ level are not shown because they are very similar). Here it is evident that the most important contribution comes from the $O_3(0\,1\,1 \leftrightharpoons 0\,2\,0)$+$M$ stretching-to-bending collisional transition which transfers energy from/to $O_3(0\,2\,0)$ level. Even though this is not a resonant transition, it remains unusually balanced up to 75 km as stated above. At this height, $O_3(0\,1\,1 \leftrightharpoons 0\,2\,0)$+O collisions increase significantly showing a similar upward imbalance as the one described for O_3+M collisions, which supports the previous assessment regarding to the $O_3(0\,v_2\,0)$ overpopulation. Below 55 km, all transitions are balanced but the $O_3(0\,2\,1 \leftrightharpoons 0\,1\,1)$+$M$ pure-bending transition which presents a noticeable imbalance in the downward

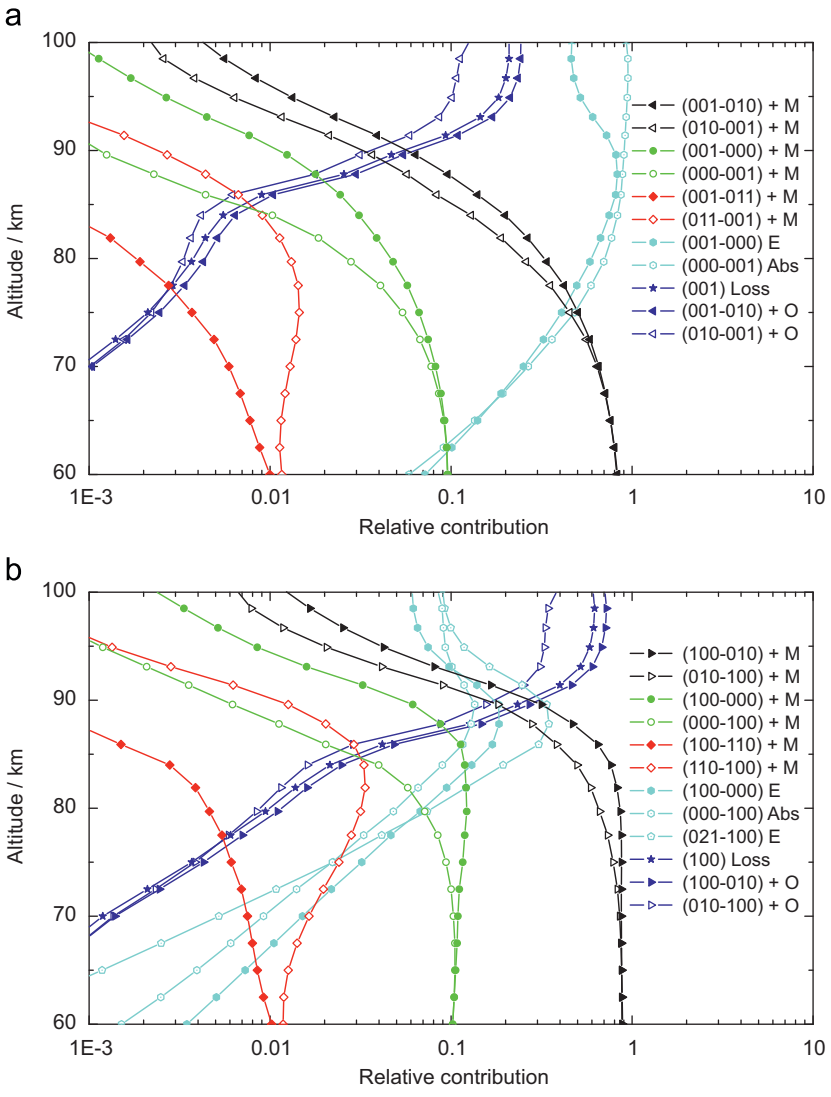

Fig. 8. Same as in Fig. 6 but for $O_3(0\,0\,1)$ level (panel a) and for $O_3(1\,0\,0)$ level (panel b). Star symbols represent the chemical loss process.

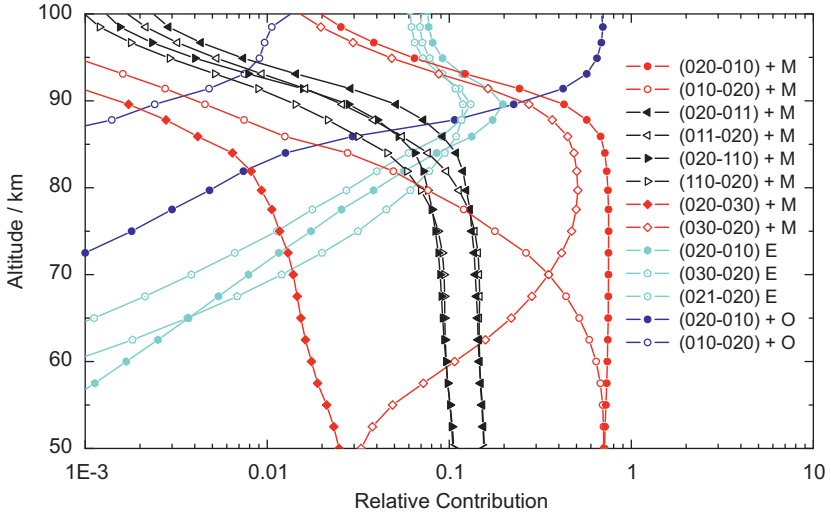

Fig. 9. Same as in Fig. 6 but for $O_3(0\,2\,0)$ level.

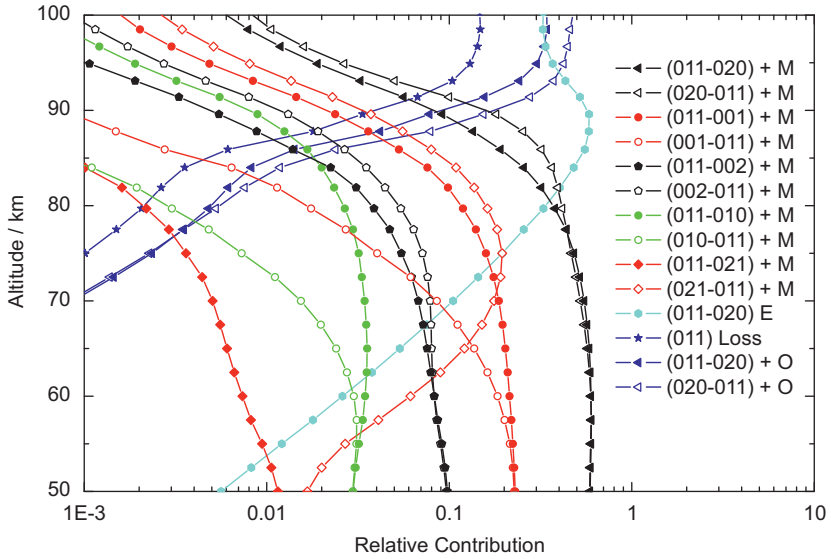

Fig. 10. Same as in Fig. 8 but for $O_3(0\,1\,1)$ level.

direction compared to the other transitions. Because radiative processes surpass $O_3(0\,2\,1 \rightarrow 0\,1\,1)$+*M* transition only above 75 km, the original T_{vib} departure is once again a consequence of the non-LTE population that the $O_3(0\,2\,1)$ level already has at this altitude.

5.3. Appearance of non-LTE for fundamental levels

After ozone is produced in the excited states by the three-body recombination reaction, it deactivates through an energy cascade including chemical, radiative and collisional processes, which affect the population of the fundamental levels. With the exception of $O_3(0\,0\,1)$ level, neither absorption nor emission of infrared radiation accounts for more than a few percent of the populating or depopulating channels for the fundamental levels below 75 km. The most important contributors to the fundamental levels are always the collisional processes, which become imbalanced at different altitudes. Then, non-LTE cannot be attributed to a direct competition between collisional and radiative processes as usually stated, at least for the fundamental levels. Radiative processes are important to produce non-LTE mainly in the higher energy levels and in the ν_3 mode. The rest of the ozone energy levels depart from LTE because of the coupled mechanism controlled by collisions. For example, non-LTE on $O_3(0\,1\,0)$ level appears through an imbalanced interaction with $O_3(0\,2\,0)$ level, which is in agreement with a relaxation cascade through $O_3(0\,\nu_2\,0)$ levels.

6. Summary and concluding remarks

The new non-LTE model developed allows quantifying the contribution of each transition in the state-to-state energy transfer during the relaxation of vibrationally excited ozone after it is formed by recombination. With this new model, the altitude T_{vib} profiles were obtained for different levels, and the appearance of non-LTE for the $O_3(0\,1\,0)$, $O_3(0\,0\,1)$, $O_3(1\,0\,0)$, $O_3(0\,2\,0)$ and $O_3(0\,1\,1)$ levels was analyzed.

The results show that collisional VT processes play a key role in the energy redistribution of the vibrational excited nascent ozone even under non-LTE conditions. Even though most levels present a radiative imbalance between emission and absorption, its contribution to the kinetic law is negligible below 90 km with exception of $O_3(0\,0\,1)$ level. The most important contributors to the fundamental levels are always the collisional processes, which become imbalanced at different altitudes. Deviations from LTE populations start before radiative processes become important and non-LTE appearance cannot be attributed to a direct competition between collisional and radiative processes solely. Non-LTE appears as a consequence of the global coupling of the SSE; that is, the more energetic levels acquire non-LTE populations because for them the radiative processes produce a greater contribution, but the lower levels (including the fundamental ones) reach non-LTE conditions indirectly throughout collisional VT transitions to/from other levels which already have non-LTE populations.

The three-steps sequential departure from LTE for $O_3(0\,1\,0)$, $O_3(0\,0\,1)$ and $O_3(1\,0\,0)$ levels is a consequence of the predominant energy flow through mode ν_2 in the relaxation cascade. The first fundamental level that reaches non-LTE at 65 km is $O_3(0\,1\,0)$ level throughout its direct connection to $O_3(0\,2\,0)$ level, which is already in non-LTE at this altitude. Because $O_3(0\,0\,1)$ and $O_3(1\,0\,0)$ levels are strongly coupled and their principal contributor is the stretching-to-bending transition from/to $O_3(0\,1\,0)$ level, whenever the last one reaches non-LTE, the others go along with it. Only above 70 km, the radiative processes for $O_3(0\,0\,1)$ level become important enough to produce an imbalance in the stretching-to-bending transitions which differentiate T_{vib} from the vibrational temperature value for mode ν_2, but the strong Coriolis-coupling prevents a further distinction between $O_3(0\,0\,1)$ and $O_3(1\,0\,0)$ levels until 75 km where radiation is clearly the most important contributor in the ν_3 fundamental band.

The $O_3(0\,\nu_2\,0)$ overpopulation is a consequence of the great impact that the stretching-to-bending collisional transitions have on the energy flow throughout the relaxation cascade. Once energy reaches one of these levels, it can no longer return to the stretching modes unless it follows an upward transition. In the presented mechanism, this is only possible when the $O_3(0\,\nu_2\,0)$ overpopulation is large enough to offsets the energy difference between levels. SSH theory allows the calculation of bending-to-stretching rate constants (k_{2D}) for high-energy levels transitions, which have not been measured because they do not involve $O_3(0\,1\,0)$ level. k_{2D} values are of the same order of magnitude as k_D values in such a way that its inclusion will represent a non-negligible contribution compared to the transitions included so

far in the model, mainly when an $O_3(0\,\nu_2\,0)$ overpopulation exists. In an upcoming work, a coupled mechanism including SSH k_{2D} rate constants will be used to assess the impact of bending-to-stretching transitions on the vibrational temperature of the ozone fundamental levels and the lower hot levels.

Acknowledgements

The authors would like to thank CONICET and SeCyT (UNC) for partial support for this work and B. Funke for fruitful discussions. R.P. Fernández thanks CONICET for a graduate fellowship and DAAD for a research fellowship at Juelich Research Center, Germany. B.M. Toselli thanks Prof. John Barker for providing the original version of the SSH code and for helpful discussions. We also thank an anonymous reviewer for his/her corrections, suggestions and constructive comments.

References

Barker, J., 2001. Personal communication.

Brasseur, G., Solomon, S., 1984. Aeronomy of the Middle Atmosphere. D. Reidel Publishing Company, The Netherlands.

Doyennette, L., Ménard, J., Ménard-Bourcin, F., 1990. Coriolis assisted intermode vibrational energy transfers in O_3–M gas mixtures (M = O_2, N_2, Ar) from infrared double-resonance measurements. Chemical Physics Letters 170, 197–200.

Doyennette, L., Boursier, C., Ménard, J., Ménard-Bourcin, F., 1992. $\nu_1 \leftrightarrow \nu_3$ Coriolis-assisted intermode transfers in O_3–M gas mixtures (M = O_2 and N_2) in the temperature range 200–300 K from IR double-resonance measurements. Chemical Physics Letters 197, 157–160.

Edwards, D.P., López-Puertas, M., López-Valverde, M.A., 1993. Non-local thermodynamic equilibrium studies of the 15-μm bands of CO_2 for atmospheric remote sensing. Journal of Geophysical Research 98 (D8), 14955–14977.

European Space Agency, Envisat, 2000. MIPAS: An Instrument for Atmospheric Chemistry and Climate Research. ESA Publication Division, ESTEC, Noordwijk, The Netherlands.

Fernández, R.P., Palancar, G.G., Madronich, S., Toselli, B.M., 2007. Photolysis rate coefficients in the upper atmosphere: effect of line-by-line calculations of the O_2 absorption cross section in the Schumann–Runge bands. Journal of Quantitative Spectroscopy and Radiative Transfer 104, 1–11.

Fischer, H., Oelhaf, H., 1996. Remote sensing of vertical profiles of atmospheric trace constituents with MIPAS limb-emission spectrometers. Applied Optics 35 (16), 2787–2796.

Funke, B., Martín-Torres, F.J., López-Puertas, M., Höpfner, M., Hase, F., López-Valverde, M.Á., García-Comas, M., 2002. A generic non-LTE population model for MIPAS-ENVISAT data analysis. Geophysical Research Abstracts, 4 abstracts of the contribution of the European Geophysical Society. CD-ROM. ISSN:1029-7006.

Gil-López, S., López-Puertas, M., Kaufmann, M., Funke, B., García-Comas, M., Koukouli, M.E., Glatthor, N., Grabowski, U., Höpfner, M., Stiller, G.P., von Clarmann, T., 2005. Retrieval of stratospheric and mesospheric O_3 from high resolution MIPAS spectra at 15 and 10 μm. Advances in Space Research 36, 943–951.

Goussev, O., 2002. Non-LTE diagnostics of the infrared observations of the planetary atmosphere. Dissertation an der Fakultät für Physik der Ludwing-Maximilians-Universität, München.

Herzberg, G., 1991. Molecular Spectra and Molecular Structure: II. Infrared and Raman Spectra of Polyatomic Molecules, reprint ed. Krieger Publishing Company, Malabar, FL, USA.

Hippler, H., Rahn, R., Troe, J., 1990. Temperature and pressure dependence of ozone formation rates in the range 1–1000 mbar and 90–370 K. Journal of Chemical Physics 93, 6560–6569.

Kaufmann, M., Gusev, O.A., Grossmann, K.U., Martín-Torres, F.J., Marsh, D.R., Kutepov, A.A., 2003. Satellite observations of daytime and nighttime ozone in the mesosphere and lower thermosphere. Journal of Geophysical Research 108 (D9), 4272.

Kaufmann, M., Gil-López, S., López-Puertas, M., Funke, B., García-Comas, M., Glatthor, N., Grabowski, U., Höpfner, M., Stiller, G.P., von Clarmann, T., Koukouli, M.E., Hoffmann, L., Riese, M., 2006. Vibrationally excited ozone in the middle atmosphere. Journal of Atmospheric and Solar-Terrestrial Physics 68, 202–212.

Lambert, J.D., 1977. Vibrational and Rotational Relaxation in Gasses. Clarendon Press.

López-Puertas, M., Taylor, F.W., 2001. Non-LTE Radiative Transfer in the Atmosphere. World Scientific, Singapore.

Manuilova, R.O., Shved, G.M., 1992. The 4.8 and 9.6 μm O_3 band emissions in the middle atmosphere. Journal of Atmospheric and Terrestrial Physics 54 (9), 1149–1168.

Manuilova, R.O., Gusev, O.A., Kutepov, A.A., von Clarmann, T., Oelhaf, H., Stiller, G.P., Wegner, A., López-Puertas, M., Martín-Torres, F.J., Zaragoza, G., Flaud, J.-M., 1998. Modelling of non-LTE limb spectra of i.r. ozone bands for the MIPAS space experiment. Journal of Quantitative Spectroscopy and Radiative Transfer 59, 405–422.

Marsh, D., Smith, A.K., Brasseur, G., Kaufmann, M., Gossmann, K.U., 2001. The existence of a tertiary ozone maximum in the high-latitude middle mesosphere. Geophysical Research Letters 28, 4531–4534.

Ménard, J., Doyennette, L., Ménard-Bourcin, F., 1992. Vibrational relaxation of ozone in O_3–O_2 and O_3–N_2 gas mixtures from infrared double-resonance measurements in the 200–300 K temperature range. Journal of Chemical Physics 96 (8), 5773–5780.

Ménard-Bourcin, F., Doyennette, L., Ménard, J., 1990. Vibrational energy transfer in ozone from infrared double-resonance measurements. Journal of Chemical Physics 92 (7), 4212–4221.

Ménard-Bourcin, F., Ménard, J., Doyennette, L., 1991. Vibrational relaxation of ozone in O_3–O_2 and O_3–N_2 gas mixtures from infrared double-resonance measurements. Journal of Chemical Physics 94 (3), 1875–1881.

Ménard-Bourcin, F., Doyennette, L., Ménard, J., 1994. Vibrational energy transfers in ozone excited into the (101) state from infrared double-resonance measurements. Journal of Chemical Physics 101 (10), 8636–8645.

Mlynczak, M.G., Drayson, S.R., 1990a. Calculation of infrared limb emission by ozone in the terrestrial middle atmosphere: 1. Source functions. Journal of Geophysical Research 95 (D10), 16497–16511.

Mlynczak, M.G., Drayson, S.R., 1990b. Calculation of infrared limb emission by ozone in the terrestrial middle atmosphere: 2. Emission calculations. Journal of Geophysical Research 95 (D10), 16513–16521.

Mlynczak, M.G., Zhou, D.K., 1998. Kinetic and spectroscopic requirements for the measurement of mesospheric ozone at 9.6 μm under non-LTE conditions. Geophysical Research Letters 25 (5), 639–642.

Rawlins, W.T., Armstrong, R.A., 1987. Dynamics of vibrationally excited ozone formed by three-body recombination. I. Spectroscopy. Journal of Chemical Physics 87 (9), 5202–5208.

Rawlins, W.T., Caledonia, G.E., Armstrong, R.A., 1987. Dynamics of vibrationally excited ozone formed by three-body recombination reaction. II. Kinetics and mechanism. Journal of Chemical Physics 87, 5209.

Rothman, L.S., Jacquemart, D., Barbe, A., Benner, D.C., Birk, M., Brown, L.R., Carleer, M.R., Chackerian, C., Chance, K., Coudert, L.H., Dana, V., Devi, V.M., Flaud, J.M., Gamache, R.R., Goldman, A., Hartmann, J.-M., Jucks, K.W., Maki, A.G., Mandin, J.-Y., Massie, S.T., Orphal, J., Perrin, A., Rinsland, C.P., Smith, M.A.H., Tennyson, J., Tolchenov, R.N., Toth, R.A., Vander Auwera, J., Varanasi, P., Wagner, G., 2005. The HITRAN 2004 molecular spectroscopic database. Journal of Quantitative Spectroscopy and Radiative Transfer 96, 139–204.

Schwartz, R.N., Slawsky, Z.I., Herzfeld, K.F., 1952. Calculation of vibrational relaxation times in gases. Journal of Chemical Physics 20, 1591.

Steinfeld, J.I., Gamache, R.R., 1998. Energy transfer and inelastic collisions in ozone. Spectrochimica Acta, Part A 54, 65–76.

West, G.A., Weston, R.E., Flynn, G.W., 1976. Deactivation of vibrationally excited ozone by $O(^3P)$ atoms. Chemical Physics Letters 42, 488–493.

West, G.A., Weston, R.E., Flynn, G.W., 1978. The influence of reactant vibrational excitation on the $O(^3P_J)$+O_3^* bimolecular reaction rate. Chemical Physics Letters 56, 429–433.

Wintersteiner, P.P., Picard, R.H., Aharma, R.D., Winick, J.R., Joseph, R.A., 1992. Line-by-line radiative excitation model for the non-equilibrium atmosphere: application to CO_2 15-μm emission. Journal of Geophysical Research 97 (D16), 18083–18117.